JOURNAL OF MOLECULAR SPECTROSCOPY **128,** 108–116 (1988)

Pressure Broadening of the Millimeter and Submillimeter Wave Spectra of Nitric Acid by Oxygen and Nitrogen[1]

THOMAS M. GOYETTE, WILLIAM L. EBENSTEIN, AND FRANK C. DE LUCIA

Department of Physics, Duke University, Durham, North Carolina 27706

AND

PAUL HELMINGER

Department of Physics, University of South Alabama, Mobile, Alabama 36688

The pressure broadening coefficients for nitric acid (HNO_3) interacting with oxygen (O_2) and nitrogen (N_2) have been measured for 16 transitions in the millimeter and submillimeter region. These transitions represent a good selection of the strong lines in the rotational spectrum of this species and make possible a systematic comparison with earlier theoretical calculations. For broadening by both oxygen and nitrogen we find larger coefficients than predicted by theory. In addition, the state to state variation is higher than calculated, especially for oxygen broadening for which the calculation shows essentially no state to state variation. © 1988 Academic Press, Inc.

I. INTRODUCTION

Pressure broadening coefficients are of both fundamental and practical importance. They are intimately connected with the intermolecular potential of collision dynamics and are necessary for many applications which involve the emission and propagation of electromagnetic radiation. Among the latter, many of the most important are related to problems associated with radiative transfer and remote sensing in the terrestrial atmosphere and the interstellar medium.

In this paper we report the pressure broadening coefficients for nitric acid (HNO_3) broadened by both oxygen (O_2) and nitrogen (N_2) for 16 transitions in the millimeter and submillimeter (mm/submm) spectral region. These cover a wide range of quantum states and make possible a systematic comparison with the results of earlier theoretical calculations based on Anderson theory. Since among vibrational states variations in molecular multipole moments and rotational energy level structures are expected to be small compared with experimental or theoretical uncertainties, these results should be directly applicable in the infrared.

II. EXPERIMENTAL DETAILS

A new broadband mm/submm spectrometer based upon YIG oscillator, TWT amplifier, and helium temperature detector technology was used for these measurements.

[1] Support provided by NASA Grant NSG-7540. Construction of the broadband spectrometer was supported by ARO Instrumentation Grant DAAD29-83-G-0047.

0022-2852/88 $3.00

It is shown schematically in Fig. 1. In this system a DEC PDP11/23 computer was used to convert operator-entered frequency range and sweep duration into instructions for a programmable HP3335A frequency synthesizer. The computer also phase locked the 10- to 15-GHz YIG oscillator to a harmonic of the synthesizer frequency. After frequency multiplication, the power was amplified to ~1 W by a Hughes 26- to 40-GHz TWT amplifier and matched onto a harmonic generator (*1, 2*). The resulting mm/submm power was propagated quasi-optically through the sample cell and detected by an InSb detector operating at 1.5 K. The Pyrex cell was 10 cm in diameter, 1 m long, and capped with polyethylene windows. Pressure was measured with a MKS capacitance manometer with 0.1-mTorr resolution. In order to reduce the concentration of water vapor in the nitric acid sample, the nitric acid was obtained from the vapor of a mixture of nitric and sulfuric acids. The oxygen and nitrogen were obtained from commercial sources and were better than 99.5% pure.

Data were recorded in the "true lineshape" mode in which the microwave frequency was swept rapidly through the absorption line. The bandwidth of the amplifiers and signal digitizers was large enough so that all significant Fourier components were retained. Because microwave spectroscopy is a coherent technique in which the coherence length of the source is much longer than the path to the detector, interference effects cause power variations with frequency. In our free space propagation environment these variations were minimized by adjustment of optical components. The data were digitized and stored by the computer. Because most of the data were in the regime in which the contribution of the Doppler broadening to the observed linewidth was small and because the large amount of data would have made fitting a Voigt profile very time consuming, the digitized data were fit to a Lorentzian lineshape with provision

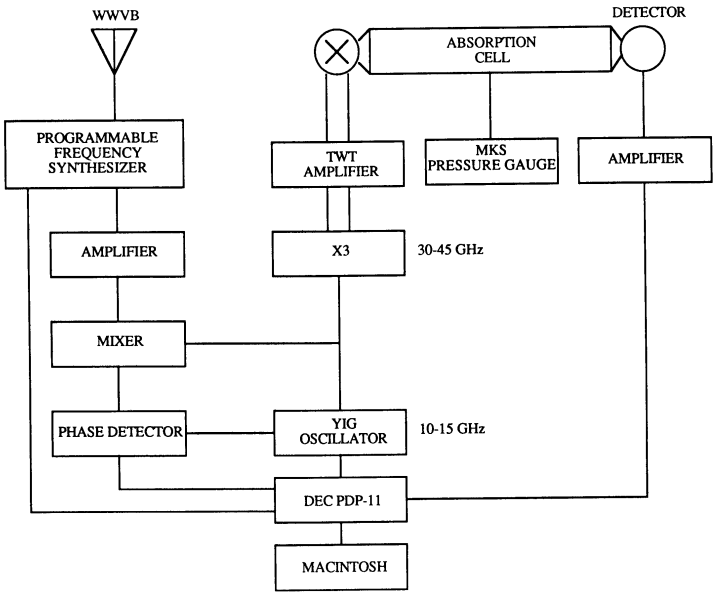

FIG. 1. Block diagram of experimental apparatus.

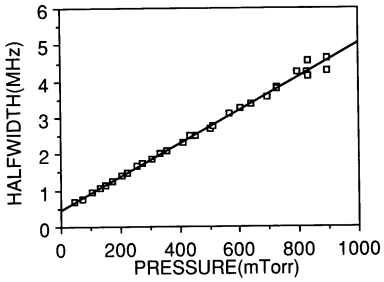

FIG. 2. Experimental data for the $19_{3,16}$–$18_{3,15}$ transition of HNO_3 broadened by N_2.

for both linear and quadratic terms in the baseline. A small correction for the contribution of the Doppler broadening was subtracted off via

$$\Delta\nu_p = [\Delta\nu_0^2 - \Delta\nu_d^2]^{1/2}, \tag{1}$$

where $\Delta\nu_p$ is the pressure-broadened linewidth, $\Delta\nu_0$ is the observed linewidth, and $\Delta\nu_d$ is the Doppler linewidth (*3*).

III. RESULTS

Data were recorded for each transition at about 25 different pressures in the range 100 to 1000 mTorr. The high pressure limit was imposed because of the increasing difficulty of deconvoluting the progressively broader lines from the power fluctuations in the system. In each case approximately 10 mTorr of HNO_3 was first introduced into the cell and the foreign gas was added incrementally. Figures 2 and 3 are representative of the best and worst of these data. Each pressure broadening coefficient was obtained from a least-squares fit to the data with the data points weighted inversely with the square of the pressure. This is based on the assumption that the accuracy of the measured half-widths was inversely proportional to their widths. Since the measurements at higher pressure are more subject to systematic errors, the lower 75% of the points were analyzed separately to see if any significantly different results would be obtained. In each case, the results were consistent and in good agreement with the analysis of the full data set.

Table I shows the experimental results. Listed first in this table are the quadruply degenerate *a*- and *b*-type transitions that result from the selection rules among the

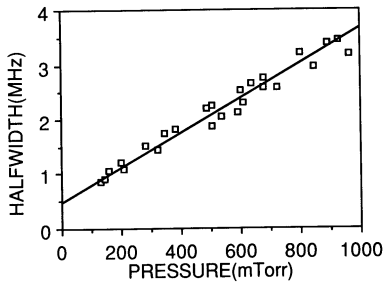

FIG. 3. Experimental data for the $29_{0,29}$–$28_{0,28}$ transition of HNO_3 broadened by O_2.

TABLE I

Broadening Parameters of HNO_3 Broadened by N_2 and O_2

Transition $J'_{K'_-K'_+}$-$J''_{K''_-K''_+}$	Frequency (MHz)	$\gamma(N_2)$ (MHz/Torr)	$\gamma(O_2)$ (MHz/Torr)
	Degenerate States		
$14_{4\,10}$-$13_{4\,9}$	231777.605	4.96 ±0.09[a]	3.24 ±0.04
$18_{0\,18}$-$17_{0\,17}$	231627.279	4.57 ±0.09	2.97 ±0.06
$19_{3\,16}$-$18_{3\,15}$	281782.006	4.59 ±0.03	3.26 ±0.04
$22_{0\,22}$-$21_{0\,21}$	281685.373	4.19 ±0.04	2.85 ±0.10
$22_{7\,15}$-$21_{7\,14}$	369487.272	4.62 ±0.05	3.25 ±0.04
$26_{9\,17}$-$25_{9\,16}$	444556.306	4.40 ±0.10	3.02 ±0.08
$27_{9\,18}$-$26_{9\,17}$	457042.054	4.27 ±0.07	2.93 ±0.04
$29_{0\,29}$-$28_{0\,28}$	369257.890	4.03 ±0.08	3.19 ±0.11
$35_{0\,35}$-$34_{0\,34}$	444283.608	4.08 ±0.04	2.99 ±0.03
$36_{0\,36}$-$35_{0\,35}$	456784.097	4.21 ±0.06	2.99 ±0.07
	Nondegenerate States		
$11_{9\,3}$-$10_{9\,2}$	235167.573	4.62 ±0.10	3.36 ±0.06
$12_{6\,6}$-$11_{6\,5}$	232178.597	5.30 ±0.14	3.54 ±0.10
$13_{11\,2}$-$12_{11\,1}$	284871.069	4.87 ±0.16	3.42 ±0.10
$14_{8\,6}$-$13_{8\,5}$	283003.022	4.88 ±0.10	3.50 ±0.06
$18_{12\,7}$-$17_{12\,6}$	370541.181	4.77 ±0.14	3.14 ±0.07
$20_{15\,5}$-$19_{15\,4}$	453822.024	3.90 ±0.11	3.17 ±0.09

a. Uncertainties are one standard deviation from the fit.

energy levels J_{K_-,K_+} and J_{K_-+1,K_+} that are doubly degenerate for large values of K_+. These lines are the strongest in this spectral region, and therefore the most significant for many applications, both because of the degeneracy and because of their large transition moments. In order to simplify the table, only the quantum numbers of the strong *a*-type transition that connect the levels labeled by the smaller values of K_- were used. In the second part of the table are listed the lines for which the asymmetry has lifted the degeneracy. Although these are weaker, they were chosen so that systematic variations in pressure broadening parameters could be investigated over a wider range of states.

Brockman *et al.* (*4*) have used a diode laser spectrometer to investigate the infrared spectrum of HNO_3 around 11 μm. In their deconvolution of those data, they deduced on the average a pressure broadening parameter for HNO_3–N_2 of 5.2 ± 0.5 MHz/Torr. This result is generally consistent with the data in Table I.

The listed statistical uncertainties are one standard deviation and are taken directly from the least-squares fit. These are included primarily to serve as an indication of the relative quality of the experimental data. It is well known that pressure broadening experiments are fraught with systematic effects. Some of these may be systematic for the whole experiment, others only for a particular transition or measurement. As we

will show below, the pressure broadening coefficients for many of the transitions can be fit by a simple smooth line to about 2% accuracy. This indicates that the differences among transitions reported here are significant at about the 2% level. Overall systematic effects associated with the experiment are probably larger.

III. THEORETICAL CONSIDERATIONS

Anderson theory (*5*), as expanded by Tsao and Curnutte (*6*), has been used by a number of workers for the purpose of calculating pressure broadening parameters. In the notation of Benedict and Kaplan (*7, 8*), the key expressions are

$$\gamma_{if}^{0} = (nv/2c)[\sum_{J_2} \rho_{J_2} (b_{if,J_2})^2], \tag{2}$$

where γ_{if}^{0} is the pressure broadening parameter, the b_{if,J_2} are the partial collision diameters, n is the number density of colliding molecules, v is the mean collision velocity, and ρ_{J_2} is the fraction of colliding molecules in the state J_2. The partial collision diameter is calculated via

$$S(b) = A_{DQ}^{6} b^{-6} [\sum_{i',J_2'} D(i,i') \cdot Q(J_2,J_2') \cdot f_2(k) + \sum_{f',J_2'} D(f,f') \cdot Q(J_2,J_2') \cdot f_2(k)] \tag{3}$$

and

$$b_{if,J_2}^{2} = b_0^2 \{1 + A_{DQ}^{6} b_0^{-6} [\sum_{i',J_2'} D(i,i') \cdot Q(J_2,J_2') \cdot F_2(k_0) + \sum_{f',J_2'} D(f,f') \cdot Q(J_2,J_2') \cdot F_2(k_0)]\}, \tag{4}$$

where b_0 is the value of b for which $S(b) = 1$, or b_m, whichever is greater,

$$A_{DQ} = [(8\pi/45)(\mu q/hv)^2]^{1/6}, \tag{5}$$

$f_2(k)$ and $F_2(k_0)$ are functions related to the energy defect in the collisional process and tabulated in Ref. (*6*), the $Q(J_2, J_2')$ are the quadrupole transition probabilities for linear molecules, and the $D(i, i')$ and $D(f, f')$ are the electric dipole transition probabilities for an asymmetric rotor.

It is useful to note that in the limit the dipole–quadrupole interaction is small, $b_0 = b_m$, and the theory reduces to a hard sphere theory in which all transitions have the same pressure broadening coefficient. In addition, $f_2(k)$ and $F_2(k)$ remain within 90% of their resonant values of 1.0 and 0.5, respectively, until $k = 2\pi b \Delta E/hv$ reaches about 2.5. Thus, for fairly heavy molecules like HNO_3, pressure broadening should appear to be "classical," with smooth variations in pressure broadening parameters with increments in quantum numbers. Although Anderson theory is only one of many possible theories, most have a similar physical basis and the discussion above is rather general.

IV. COMPARISON BETWEEN EXPERIMENT AND THEORY

Tejwani and Yeung (*9*) have done an extensive calculation based on Anderson theory of the pressure broadening of HNO_3 by both O_2 and N_2. In that work they performed a calculation based on the dipole–quadrupole interaction. Although their specific interest was the ν_2 infrared band, the calculations should be equally valid for

other bands, including the pure rotational transitions. Variations in dipole and quadrupole moments and rotational energy level spacing should be insignificant in comparison with uncertainties in the value of the molecular quadrupole moment, neglect of other higher order interactions, and the fundamental approximations inherent in the theory.

It is worth first considering what differences might be expected between collisions of nitric acid and either O_2 or N_2. Although the ground electronic states of N_2 and O_2 are $^1\Sigma$ and $^3\Sigma$, respectively, the selection rules among the triplet states are such that the quadrupolar transition frequencies are essentially unchanged. Thus it would appear that in the context of Anderson theory the major difference between broadening by O_2 and N_2 would be a result of the significantly larger molecular quadrupole moment of N_2.

Figure 4 shows our experimental results for HNO_3–N_2 broadening. In this graph the linewidth parameters are plotted against $J + K_+$ for the upper state of the transitions. All but six of the observed transitions are members of the strong quadruply degenerate $\Delta J = 1$ transitions discussed above and these are plotted as squares on the figure. Over this range of states, which is representative of the strong transitions in the HNO_3, the smooth empirical line represents the observed data to about 2% in a region in which it varies by more than 30%. This functional dependence was found as a result of a contour search for a simple relation among the pressure broadening coefficients. Three more, plotted as triangles, are similar transitions, but ones in which the lifting of the degeneracy has split the levels by <1 GHz. The remaining three transitions, plotted as diamonds, arise from levels far from the region of K_+ degeneracy.

Figure 5 shows a comparison of the theoretical and experimental results for HNO_3 broadened by N_2. The theoretical values are high, but systematically related to the variation in the experimental data as shown by the straight line of unity slope plotted on the graph. The intercept of this line shows that increasing all of the theoretical values by ~0.7 MHz/Torr would substantially improve the agreement. However, the deviations between experiment and theory would still be several times the deviation between the empirical line of Fig. 4 and the experimental data. This is especially true for the larger pressure broadening coefficients, for which the quantum mechanical features of the problem are more apparent.

Figure 6 shows our experimental results for the HNO_3–O_2 pressure broadening

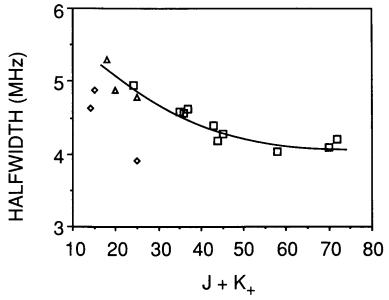

FIG. 4. Experimentally observed pressure broadening coefficients for HNO_3–N_2 plotted versus $J + K_+$. The smooth curve and points are discussed in the text.

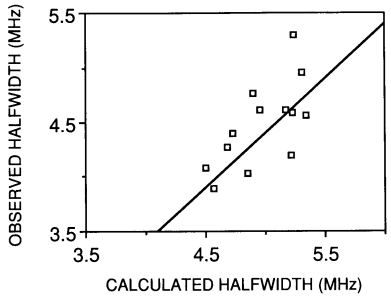

FIG. 5. A comparison of experimental and theoretical pressure broadening coefficients for HNO_3–N_2 collisions.

coefficients. Again, the squares are the quadruply degenerate transitions, the triangles the moderately split transitions, and the diamonds the widely split transitions. Figure 7 shows the correlation between experimental and theoretical values of the pressure broadening parameter on a line by line basis. These figures reveal several details. First, the theoretical results are systematically lower and essentially constant, and second, at higher values of $J + K_+$ the experimental values are also essentially constant. These results further show that there is no obvious correlation between the theoretical and experimental results.

Much of the above is understandable at least in qualitative terms on the basis of the form of Anderson theory and its implementation. Tejwani and Yeung explicitly considered only the quadrupole–dipole interaction in their calculations because higher order interaction parameters were unknown. In that formulation Anderson theory has two adjustable or poorly known parameters, the molecular quadrupole moment q_m of the collision partner and the minimum impact parameter b_m. The dipole moment of HNO_3 is well known.

In the theoretical calculations the HNO_3–O_2 system approaches the limit in which the relative sizes of q_m and b_m are such that b_m dominates, and all transitions have similar pressure broadening coefficients. However, the experimental results show that significantly more variation in pressure broadening parameter exists. It is well known that the introduction of b_m into Anderson theory in a large measure is to compensate

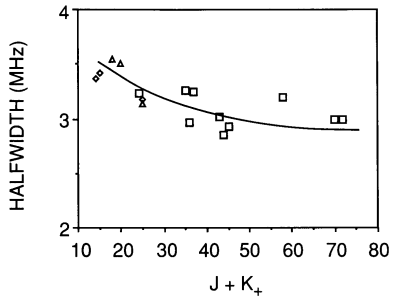

FIG. 6. Experimentally observed pressure broadening coefficients for HNO_3–O_2 plotted versus $J + K_+$. The smooth curve and points are discussed in the text.

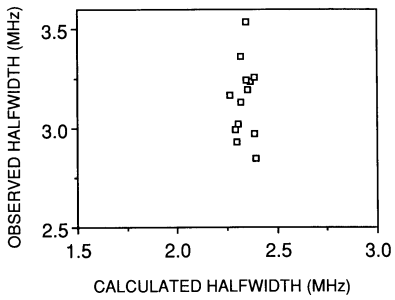

FIG. 7. A comparison of experimental and theoretical pressure broadening coefficients for HNO_3–O_2 collisions.

for the omission of unknown higher order interaction terms in the multipole expansion that become significant at small intermolecular distances. Presumably, if it were possible to include these effects a better correlation between experiment and theory would occur. Alternatively, a simple readjustment of b_m and q_m would result in an improved agreement, if for no other reason than a general upward adjustment in the theoretical values. Both the experimental data and theoretical calculations for HNO_3–N_2 collisions show much more variation than the HNO_3–O_2 case. This is to be expected because q_m is considerably larger for N_2 than for O_2 and as a result the quantum mechanical nature of the problem is more apparent.

It is illuminating to compare these results with the results of a theoretical calculation of H_2O–N_2 and H_2O–O_2 pressure broadening coefficients by Benedict and Kaplan (*7, 8*). The most significant difference between the HNO_3 and H_2O results is the much greater variation in calculated pressure broadening parameters for the H_2O case. This can be understood in the context of the energy defect terms $f(k)$ in Anderson theory. For HNO_3 the rotational constants are such that for thermally populated levels even at high quantum number, the transition frequencies are still small in comparison to kT. However, the rotational constants of H_2O are very large, and for many states the energy defect term will make a significant contribution to the calculation.

In addition, for the case of H_2O–N_2, the molecular quadrupole moment q_m of N_2 was adjusted so that the calculated pressure broadening coefficient matched exactly the one reliably known experimental value at this time, the microwave measurement of the $6_{1,6}$–$5_{2,3}$ transition. This resulted in a q_m that was large in comparison to values obtained from other sources. However, the argument was made that this procedure compensated for other higher order interactions that were not included in the calculation. It would appear that if an appropriate experimental data point had been available prior to the Anderson theory calculations for HNO_3 in Ref. (9), significantly better agreement between experiment and theory could have been obtained.

V. CONCLUSIONS

This work represents one of the few studies of pressure broadening in the mm/submm spectral region that contains a wide enough range of data to make possible systematic comparisons with the results of theoretical calculations. Nitric acid is a good subject for such a study both because of its fundamental significance and because

its strong transitions in this spectral region give easy access to a range of quantum states. It was found that the pressure broadening coefficients for collisions with N_2 were both larger and had a substantially wider range of values than the coefficients for collisions with O_2. This general result is to be expected based upon the relative sizes of the molecular quadrupole moments of the two collision partners. For the strong transitions reported here it was shown that the observed pressure broadening coefficients had a smooth functional dependence on the quantum numbers, but that substantial difference existed between the experimental results and previous Anderson theory calculations. Since these calculations had to be based on molecular parameters that were marginally known at best, it would be very interesting to investigate how good an agreement could be obtained between theory and experiment if these parameters could be adjusted to fit the experimental data. It would also be interesting to extend this comparison to weaker and low J lines for which larger variations in pressure broadening might be expected.

RECEIVED: August 31, 1987

REFERENCES

1. W. C. KING AND W. GORDY, *Phys. Rev.* **90,** 319–320 (1953).
2. P. HELMINGER, J. K. MESSER, AND F. C. DE LUCIA, *Appl. Phys. Lett.* **42,** 309–310 (1983).
3. C. H. TOWNES AND A. L. SCHAWLOW, "Microwave Spectroscopy," Dover, New York, 1975.
4. P. BROCKMAN, C. H. BAIR, AND F. ALLARIO, *J. Appl. Optics* **17,** 91–100 (1978).
5. P. W. ANDERSON, *Phys. Rev.* **76,** 647–661 (1949).
6. C. J. TSAO AND B. CURNUTTE, *J. Quant. Spectrosc. Radiat. Transfer* **2,** 41–91 (1962).
7. W. S. BENEDICT AND L. D. KAPLAN, *J. Chem. Phys.* **30,** 388–399 (1959).
8. W. S. BENEDICT AND L. D. KAPLAN, *J. Quant. Spectrosc. Radiat. Transfer* **4,** 453–469 (1964).
9. G. D. T. TEJWANI AND E. S. YEUNG, *J. Chem. Phys.* **68,** 2012–2013 (1978).